



ELSEVIER

Contents lists available at ScienceDirect

## Solar Energy Materials &amp; Solar Cells

journal homepage: [www.elsevier.com/locate/solmat](http://www.elsevier.com/locate/solmat)

# Solution processed thin films of non-aggregated TiO<sub>2</sub> nanoparticles prepared by mild solvothermal treatment

Young Gon Seo<sup>a</sup>, Min Ah Kim<sup>b</sup>, Hyunjung Lee<sup>b,\*</sup>, Wonmok Lee<sup>a,\*\*</sup>

<sup>a</sup> Department of Chemistry, Sejong University, 98 Gunja-Dong, Gwngjin-gu, Seoul 143-747, Republic of Korea

<sup>b</sup> Materials Science and Technology Research Division, Korea Institute of Science and Technology, 39-1 Hawolgok-dong, Seongbuk-gu, Seoul 136-791, Republic of Korea

## ARTICLE INFO

### Article history:

Received 4 November 2009

Received in revised form

18 February 2010

Accepted 3 May 2010

Available online 20 May 2010

### Keywords:

TiO<sub>2</sub> nanoparticles

Solvothermal process

Thin film

Wet coating

Inverse opal

Dye-sensitized solar cell

## ABSTRACT

In this report, non-aggregated anatase TiO<sub>2</sub> nanoparticles were synthesized by mild solvothermal process in 1-butanol. By varying solvothermal reaction temperature and time, TiO<sub>2</sub> particle size was controlled from 5.3 to 9.0 nm, while maintaining pure anatase phase and optical clearance in the concentrated dispersion (5 wt%). Spin coating of TiO<sub>2</sub> dispersions resulted in transparent thin films with thickness controllability, and it was confirmed that the mild solvothermal reaction significantly increased the refractive index of the thin films without post-thermal treatment. In addition to the fabrication of low-temperature processed thin films, the inverse opal TiO<sub>2</sub> films were also fabricated by the colloidal templating method followed by thermal calcination to reveal the improved volume shrinkage of the mesoporous TiO<sub>2</sub> films.

© 2010 Elsevier B.V. All rights reserved.

## 1. Introduction

Due to the unique photophysical properties, nanosized titania (TiO<sub>2</sub>) is an attractive material towards various applications such as solar energy harvesting [1–5], photocatalysis [6–8], antibacterial coating [9], and photonic crystals [6,10]. Among other crystalline morphologies of TiO<sub>2</sub>, anatase TiO<sub>2</sub> is regarded as the most efficient crystalline phases to be used as electron transporting materials for dye sensitized solar cell (DSSC) which are of great interest these days [1–5]. Thin films of nanocrystalline TiO<sub>2</sub> can be obtained either by dry-process [4] or wet-process [9]. Compared to dry-process, wet-process is often preferred owing to the flexibility and cost-effectiveness of the process [11]. In order to assure pure anatase TiO<sub>2</sub> nanoparticles in the thin film, the coating process is followed by calcination at the temperature below 450 °C [5]. Instead of calcination, hydrothermal [9,12], or non-aqueous solvothermal [8,13] treatment of TiO<sub>2</sub> sol at an elevated temperature can also produce highly crystalline anatase TiO<sub>2</sub> nanoparticles. The solution processability of TiO<sub>2</sub> nanoparticle such as coating property depends on its particle size, size distribution, and surface functional groups. Socolan and Sanchez [14] synthesized highly dispersed anatase TiO<sub>2</sub> nanoparticles in

organic solvent by introducing organic modifier at nanoparticle surface. The organically modified TiO<sub>2</sub> showed promising applicability to the photonic devices such as 3-D photonic crystal structure [11], and DSSC photoelectrode [5].

In this study, we investigated various solvothermal reaction conditions in order to control the particle size and the crystallinity of the organically modified TiO<sub>2</sub> nanoparticle system which can be processed into the transparent films.

## 2. Experimental

The synthesis of organically modified TiO<sub>2</sub> nanoparticle was carried out following the method reported elsewhere [14]. As-synthesized TiO<sub>2</sub> nanoparticle was redispersed in 1-butanol, which was sealed in a stainless steel bomb reactor (4744 Parr instrument). In a temperature stabilized oven, mild solvothermal reaction was carried out at the temperature ranging from 160 to 240 °C for 3–10 h, followed by precipitation and drying.

The crystal structure of TiO<sub>2</sub> powder was characterized by X-ray diffractometer (XRD, Rigaku D/Max-2500). High-resolution transmission electron microscopy (HR-TEM) (tecna F20, FEI) analyses were carried out to observe the nanoparticles' shape and morphology.

Organic contents in TiO<sub>2</sub> nanoparticles were characterized by thermogravimetric analysis (TGA, TA Instrument). The thin films of TiO<sub>2</sub> were prepared by spin coating the butanol dispersion on

\* Corresponding author. Tel.: +82 2 958 5359; fax: +82 2 958 5309.

\*\* Corresponding author. Tel.: +82 2 3408 3212; fax: +82 2 462 9954.

E-mail addresses: lhj0630@kist.re.kr (H. Lee), wonmoklee@sejong.ac.kr (W. Lee).

the pre-cleaned substrate. After spin coating, the films were dried in convection oven at 70 °C. The thicknesses and the refractive indices of the TiO<sub>2</sub> thin films were characterized by ellipsometry (SE MF-1000, Nano-view) without calcinations.

Inverse opal structures composed of TiO<sub>2</sub> nanoparticles before and after solvothermal process were prepared, and analyzed. First, the colloidal crystals exhibiting 3D opal structure with ~5 μm thickness were prepared on slide glass using narrowly dispersed polystyrene (PS) microspheres which were synthesized by standard emulsion polymerization [15]. A detailed fabrication method for the colloidal crystal is reported elsewhere [1–5]. The dispersions of TiO<sub>2</sub> nanoparticles at 5 wt% in 1-butanol were infiltrated within the colloidal crystals by spin coating at 500 rpm. Once dried in air overnight, PS colloidal crystal template was removed by calcination at 450 °C using a furnace (LK-Lab Korea). The resulting inverse opal structures were analyzed by SEM.

### 3. Results and discussion

From the previous literatures, non-aggregated TiO<sub>2</sub> nanoparticle system used in this study showed unique solution processibility toward thin film applications [11]. As-synthesized TiO<sub>2</sub> nanoparticle was obtained as a fine yellowish powder as shown in Fig. 1(a), and it was readily dispersed in 1-butanol solution up to 30 wt% without necessity for heating to promote solvation. Such an excellent dispersibility of TiO<sub>2</sub> originates from its narrow size distribution and surface modification by AcAc.

Fig. 1(b) shows the solvothermally treated dispersions at 180 °C for 3 different reaction times. Although the reaction temperature of 180 °C was regarded as a mild condition for solvothermal treatment, longer reaction time apparently caused the increased opaqueness to the dispersions. At a fixed reaction time (3 h), the temperatures above boiling point of 1-butanol (117 °C) were surveyed for each 5 wt% TiO<sub>2</sub> dispersion in 1-butanol. The solvothermally treated dispersions at 4 different reaction times are shown in Fig. 1(c). The clearance of the dispersion was maintained up to 200 °C solvothermal temperature, though the dispersions treated at 200 °C showed a slight increase in turbidity. It was found at the solvothermal temperature above 200 °C, the dispersion turned very turbid. Since the aim of this study was to improve refractive index of TiO<sub>2</sub> film while maintaining optical transparency, optimized solvothermal

condition was concluded to be the temperature of 180 °C, and reaction time of 3–5 h.

The 1-butanol dispersions of TiO<sub>2</sub> samples except for that treated at 240 °C were spin-coated on the glass slide which had been pre-cleaned by piranha solution. The concentration (5 wt%) and the spin rate (2000 rpm) have been optimized to give ~100 nm film thickness on the glass substrate or Si wafer. As shown in Fig. 1(d) and (e), all the coated TiO<sub>2</sub> films are optically clean without dewetting or any visible aggregates, exhibiting shiny reflection color depending on the thickness. Optical clarity of the solvothermally treated TiO<sub>2</sub> dispersions was further confirmed by UV–vis transmittance measurement. The TiO<sub>2</sub> dispersions of 0.5 wt% in butanol showed a good transmittance above 400 nm wavelength except that treated at 240 °C [6–8]. Similarly, the dispersions prepared at different solvothermal reaction time up to 10 h showed good transmittance above 400 nm. As shown in Table 1, the transmittance of as-synthesized sample measured at 500 nm was 97%, but it slightly decreased as solvothermal reaction time gets longer. Such a tendency is mainly attributed to the increased turbidity by solvothermal reaction. XRD data for the powdered samples revealed the characteristic peaks from pure anatase crystal. By measuring FWHM of the peaks from (1 0 1), (0 0 4), (2 0 0), (2 0 4), and (2 1 5) plane, average particle size ( $d_{ave}$ ) of each TiO<sub>2</sub> nanoparticle was calculated based on the Scherrer formula, and the calculated size was summarized in Table 1. The calculated  $d_{ave}$  clearly showed the increasing tendency of the particle size from 5.3 to 9.0 nm by increased solvothermal temperature and reaction time.

For the comparison of the particle size and the shape changes by solvothermal reaction, TiO<sub>2</sub> nanoparticles before and after solvothermal reaction were characterized by HR-TEM as shown in Fig. 2. Compared to Fig. 2(a) in which small-sized individual nanocrystals are shown, Fig. 2(b) and (c) shows the gradual increases in TiO<sub>2</sub> particle sizes by longer solvothermal reaction time. Overall, particle shapes were elliptical. Fig. 2(d) is the enlarged view of an individual nanocrystal after solvothermal treatment at 180 °C for 3 h, where anatase crystalline lattice structure is evidently shown. Although not shown, the anatase crystalline phase was again confirmed through selective area electron diffraction (SAED) on HR-TEM image of the nanocrystals.

For the characterization of organic contents in each TiO<sub>2</sub> sample, TGA thermograms of selected samples (reacted at 180 °C) were obtained as shown in Fig. 3. Every sample showed a typical weight loss below 100 °C due to evaporation of adsorbed water.

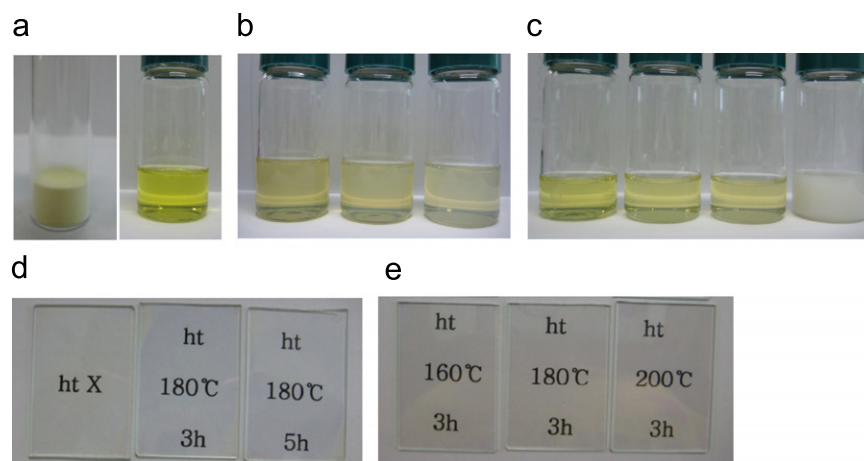


**Fig. 1.** Non-aggregated titania nanoparticles synthesized in this study (a) As-synthesized TiO<sub>2</sub> powder, and 5 wt% dispersion in 1-butanol. (b) Solvothermally treated dispersions at 180 °C for different reaction time 3, 5, and 10 h, from left. (c) Solvothermally treated dispersions for 3 h at different temperatures 160, 180, 200, and 240 °C from left. (d),(e) TiO<sub>2</sub> thin films spin-coated on the glass substrate. Hydrothermal conditions for each TiO<sub>2</sub> films are printed on the paper below each coated film showing optical clarity for all cases. All the films were obtained by spin coating 1-butanol solution of 5% TiO<sub>2</sub> at 2000 rpm.

**Table 1**  
Physical properties of TiO<sub>2</sub> nanoparticles.

Solvothermal condition	Reaction time varied at fixed temperature (180 °C)				Reaction temperature varied at fixed time (3 h)			
	0 h (as-synthesized)	3 h	5 h	10 h	160 °C	180 °C	200 °C	240 °C
Organic content (%)	30	14	13	11	x	x	x	x
Average size (nm)	5.3	8.8	9.0	9.3	8.4	8.8	8.9	x
Refractive index	1.82	1.89	1.92	x	1.85	1.88	1.91	x
Transmittance (at $\lambda=500$ nm, %)	98.2	96.9	95.4	95.3	98.2	98.3	97.7	14.4

x: not measured.

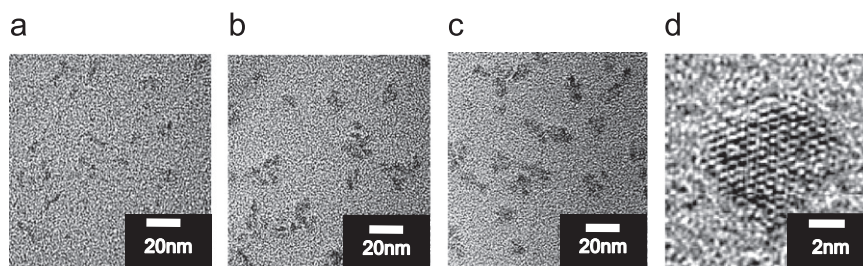


**Fig. 2.** HR-TEM images of TiO<sub>2</sub> nanocrystals obtained from solvothermal reactions at 180 °C for different reaction time. (a) As-synthesize particles, (b) after 3 h, (c) after 5 h, and (d) individual TiO<sub>2</sub> nanocrystal enlarged from (b).

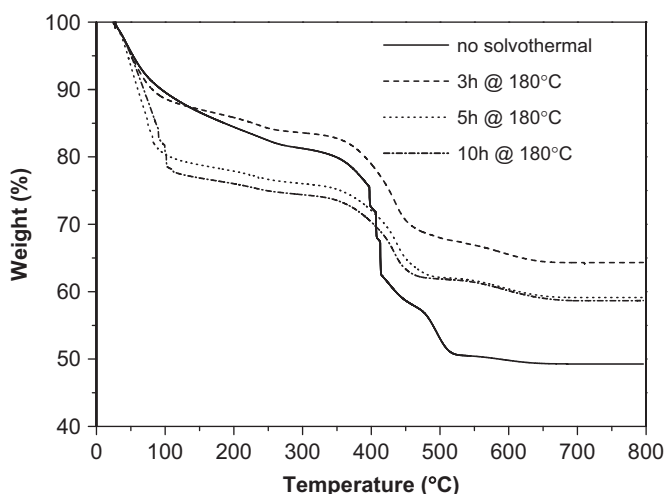


**Fig. 3.** TGA thermograms of TiO<sub>2</sub> nanocrystals obtained from solvothermal reactions at 180 °C for different reaction time.

After plateaus up to 400 °C, degradation of organic groups occurred for respective samples. Organic content of pristine TiO<sub>2</sub> sample was measured to be 30%, while those of the samples after solvothermal treatment gradually decreased down to 11%. The results are summarized in Table 1. The decrease in organic content can be attributed to the decreased surface area of TiO<sub>2</sub> nanoparticles due to the particle size growth after solvothermal reaction.

One of the most important physical properties of TiO<sub>2</sub> nanoparticle controlled by solvothermal treatment is a refractive index. As mentioned earlier, a drawback of the organically modified TiO<sub>2</sub> nanoparticle was a low refractive index (<1.8) due to high organic content. It was confirmed that refractive indices of TiO<sub>2</sub> thin films were increased by solvothermal reaction. The increased reaction time up to 5 h and the increased solvothermal temperature up to 200 °C resulted in the refractive index as high as 1.92 without loss of optical clarity of the films ( $\Delta n$  variation is shown in the supporting data).

The tapping mode AFM images on the thin film of as-synthesized TiO<sub>2</sub> nanoparticle showed very even surface with root-mean-square (rms) roughness of 1.0 nm while the film of 3 h solvothermal treated TiO<sub>2</sub> exhibited a slightly rougher surface with rms roughness of 1.7 nm without visible agglomerates. Almost no trace of dewetting or large agglomerate after spin coating was observed by AFM analyses.

Towards the photocatalytic applications, there is growing interest in the fabrication of mesoporous TiO<sub>2</sub> nanocrystals [10]. Recently, TiO<sub>2</sub> inverse opal made from polymeric colloidal crystal template was used as a light-amplified photoelectrode for DSSC [1–5]. However, the fabrication process of TiO<sub>2</sub> inverse opal includes calcinations step which accompanies a large volume shrinkage of at an elevated temperature (~450 °C) resulting in a decreased solar cell efficiency.

In this study, non-aggregated TiO<sub>2</sub> nanoparticles were fabricated into the inverse opal structures on glass substrate using polymeric colloidal crystal of PS to investigate the volume shrinkage upon calcinations. Fig. 4 shows various inverse opal structures obtained from colloidal crystal templating method. After the colloidal templates were burned off by thermal calcinations at 450 °C, it was confirmed that the inverse opal from TiO<sub>2</sub> of 5 h solvothermal treatment exhibited the lowest reduction in volume shrinkage. A reduced shrinkage upon solvothermal treatment can be attributed to a lower organic content on the surface of TiO<sub>2</sub> nanoparticles. Non-aggregated property as well as small particle size of our TiO<sub>2</sub> resulted in an excellent inverse opal formation for various PS particle sizes without significant volume shrinkage as shown in Fig. 4(d)–(f).

The inverse opal TiO<sub>2</sub> shown in Fig. 4 can be directly used as a photoelectrode for DSSC. The conductivity of TiO<sub>2</sub> particles should be increased by calcination due to elimination of organic groups, although anatase TiO<sub>2</sub> is well known n-type semiconductor material.

In summary, mild solvothermal treatments on the organically modified TiO<sub>2</sub> system resulted in the precise control of the particle size and crystallinity without significant agglomeration of the nanoparticles. The spin-coated TiO<sub>2</sub> film showed the refractive index as high as 1.91 without thermal treatment. The non-aggregated TiO<sub>2</sub> nanoparticles were successfully infiltrated into

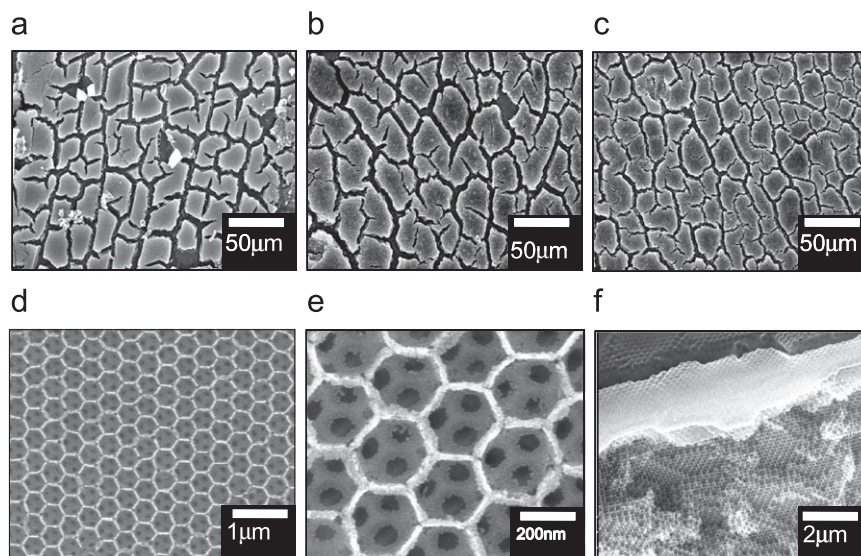


**Fig. 4.** SEM images of inverse opal films (thickness  $\sim 5 \mu\text{m}$ ) prepared using  $\text{TiO}_2$  nanoparticles with different solvothermal treatment time, (a) 0 h, (b) 3 h, and (c) 5 h. PS microsphere with 500 nm particle diameter was used for sacrificial colloidal template. Inverse opals made of PS template with different particle sizes of (d) 500 nm, (e) 350 nm, and (f) 280 nm are also shown.

colloidal crystal template, which were consequently converted to the inverse opal structure which can be directly utilized as a photoelectrode of light-amplified DSSC.

#### Acknowledgments

Authors thank Prof. Young Soo Seo in Sejong University for kind help with ellipsometry measurement. W. Lee and Y.G. Seo acknowledge the financial support by Renewable Energy Grant from KETEP (Grant no. 2008NPV08J0130302008). H. Lee acknowledges the financial support of this work by the National Research Foundation of Korea Grant funded by the Korean Government (MEST) (NRF-2009-C1AAA001-2009-0093049).

#### Appendix A. Supplementary material

Supplementary data associated with this article can be found in the online version at doi:10.1016/j.solmat.2010.05.023.

#### References

- [1] S. Nishimura, N. Abrams, B.A. Lewis, L.I. Halaoui, T.E. Mallouk, K.D. Benkstein, J. van de Lagemaat, A.J. Frank, Standing wave enhancement of red absorbance and photocurrent in dye-sensitized titanium dioxide photoelectrodes coupled to photonic crystals, *J. Am. Chem. Soc.* 125 (2003) 6306–6310.
- [2] L.I. Halaoui, N.M. Abrams, T.E. Mallouk, Increasing the conversion efficiency of dye-sensitized  $\text{TiO}_2$  photoelectrochemical cells by coupling to photonic crystals, *J. Phys. Chem. B* 109 (2005) 6334–6342.
- [3] A. Mihi, H. Miguez, Origin of light-harvesting enhancement in colloidal-photonic-crystal-based dye-sensitized solar cells, *J. Phys. Chem. B* 109 (2005) 15968–15976.
- [4] S.C. Yang, D.J. Yang, J. Kim, J.M. Hong, H.G. Kim, I.D. Kim, H. Lee, Hollow  $\text{TiO}_2$  hemispheres obtained by colloidal templating for application in dye-sensitized solar cells, *Adv. Mater.* 20 (2008) 1059–1064.
- [5] E.S. Kwak, W. Lee, N.G. Park, J. Kim, H. Lee, Compact inverse-opal electrode using non-aggregated  $\text{TiO}_2$  nanoparticles for dye-sensitized solar cells, *Adv. Func. Mater.* 19 (2009) 1093–1099.
- [6] C. Wang, Z.-X. Deng, Y. Li, The synthesis of nanocrystalline anatase and rutile titania in mixed organic media, *Inorg. Chem.* 40 (2001) 5210–5214.
- [7] A.L. Linsebigler, G. Lu, J.T. Yates, Photocatalysis on  $\text{TiO}_2$  surfaces: principles, mechanisms, and selected results, *Chem. Rev.* 95 (2002) 735–758.
- [8] J. Wu, X. Lu, L. Zhang, F. Huang, F. Xu, Dielectric constant controlled solvothermal synthesis of a  $\text{TiO}_2$  photocatalyst with tunable crystallinity: a strategy for solvent selection, *Eur. J. Inorg. Chem.* 2009 (2009) 2789–2795.
- [9] S.D. Burnside, V. Shklover, C. Barbe, P. Comte, F. Arendse, K. Brooks, M. Gratzel, Self-organization of  $\text{TiO}_2$  nanoparticles in thin films, *Chem. Mater.* 10 (1998) 2419–2425.
- [10] O.D. Velev, E.W. Kaler, Structured porous materials via colloidal crystal templating: from inorganic oxides to metals, *Adv. Mater.* 12 (2000) 531–534.
- [11] J. Yoon, W. Lee, J.-M. Caruge, M. Bawendi, E.L. Thomas, S. Kooi, P.N. Prasad, Defect-mode mirrorless lasing in dye-doped organic/inorganic hybrid one-dimensional photonic crystal, *Appl. Phys. Lett.* 88 (2006) 091102–091103.
- [12] S. Jeon, P.V. Braun, Hydrothermal synthesis of Er-doped luminescent  $\text{TiO}_2$  nanoparticles, *Chem. Mater.* 15 (2003) 1256–1263.
- [13] B. Wen, C. Liu, Y. Liu, Solvothermal synthesis of ultralong single-crystalline  $\text{TiO}_2$  nanowires, *New J. Chem.* 29 (2005) 967–971.
- [14] E. Scolan, C. Sanchez, Synthesis and characterization of surface-protected nanocrystalline titania particles, *Chem. Mater.* 10 (1998) 3217–3223.
- [15] M. Egen, R. Zentel, Tuning the properties of photonic films from polymer beads by chemistry, *Chem. Mater.* 14 (2002) 2176–2183.